International Journal of Engineering and Advanced Technology (IJEAT)
ISSN: 2249-8958 (Online), Volume-1 Issue-2, December 2011

Hybrid PWM Algorithm Based Vector Controlled Induction Motor Drive to Achieve Superior Waveform Quality

K. Satyanarayana, J. Amarnath, A. Kailasa Rao

Abstract: ***This paper presents a Hybrid PWM Algorithm Based Vector Controlled Induction Motor Drive to Achieve Superior Waveform Quality. The proposed algorithm uses six basic bus-clamping PWM (BBCPWM) sequences along with the conventional SVPWM (CSVPWM) sequence and these switching sequences have been developed by using the concept of imaginary switching times without using the angle and sector information. The proposed Hybrid PWM(HPWM) algorithm selects a suitable PWM sequence which results in lowest rms current ripple over a given sampling time interval. To validate the proposed HPWM algorithm, numerical simulation studies have been carried out and the results have been presented and compared.***

Index Terms**: *CSVPWM, BBCPWM, HPWM, Induction motor, vector control.***

I. INTRODUCTION

The high performance speed control of induction motor is based on the vector control, which is also known as field oriented control (FOC). The invention of field oriented control or vector control brought a renaissance in high performance induction motor drives. With the vector control algorithm [1], the decoupling of torque and flux control commands of the induction motor is guaranteed, and the induction motor can be controlled as a separately excited dc motor. However, the vector control algorithm uses hysteresis type current controllers for the generation of gating signals, which results in variable switching frequency operation of the inverter. To achieve constant switching frequency operation of the inverter, the conventional space vector PWM (CSVPWM) algorithm [2] has been used for vector controlled induction motor drive. The CSVPWM algorithm divides the zero state time equally among the two zero voltage vectors. By using the freedom of dividing the zero state time, various basic bus-clamping PWM (BBCPWM) algorithms can be generated as given in [3].

Manuscript published on 30 December 2011.
*** Correspondence Author (s)**
Prof. K. Satyanarayana, Professor and H.O.D. of E.E.E Department, Pragati Engineering College, Surampalem, Andhra Pradesh, India, +91 9490916767 (e-mail: snkola@gmail.com)
Dr.J.Amarnath, Professor of E.E.E Department, J.N.T. University, Hyderabad, Andhra Pradesh, India, +91 9347277771 (e-mail: amarnathjinka@yahoo.com)
Dr.A. Kailasa Rao, Professor of E.E.E Department and Director of Pragati Engineering College, Surampalem, Andhra Pradesh, India +91 8978568002 (e-mail: raoa_kailasa@yahoo.com)

In BBCPWM algorithms, the modulating signals are clamped to either positive dc bus or negative dc bus for a total period of 120 degrees for each fundamental cycle. Hence, the BBCPWM algorithms reduce the switching losses by 33.33%. Moreover, the BBCPWM algorithms reduce the total harmonic distortion (THD) during the higher modulation indices when compared with the CSVPWM algorithm. Though the conventional space vector approach offers many advantages, it requires angle and sector information to generate the gating times to the inverter. Hence, the complexity involved in the conventional space vector approach is more. To reduce the complexity involved in the conventional space vector approach, a novel voltage modulation algorithm has been proposed in [4] by using concept of effective time. By utilizing the freedom in division of active and zero state times, various possible PWM sequences have been proposed in [5]. Also, the harmonic analysis of the various PWM sequences has been carried out using the notion of stator flux ripple. The harmonic analysis of various sequences have been carried out by using the notion of current ripple in [6]-[7]. As, the algorithms proposed in [5]-[7] use the conventional space vector approach, the complexity involved is more. To reduce the complexity involved in the HPWM algorithm proposed in [5], a novel HPWM algorithm has been proposed in [8] by using the concept of imaginary switching times and verified on direct torque controlled induction motor drive.

This paper presents a simplified HPWM algorithm for vector controlled induction motor drive by using the concept of imaginary switching times and the proposed HPWM algorithm presents a Hybrid PWM algorithm based vector controlled induction motor drive to achieve superior waveform quality.

II. PROPOSED PWM SEQUENCES

The complexity involved in the conventional space vector approach is more as it requires the angle and sector information to calculate the gating times. To reduce the complexity involved, the proposed approach uses the concept of imaginary switching times. The imaginary switching times, which are proportional to the instantaneous phase voltages, can be given as in (1).

$$T_{an} = \frac{T_s}{V_{dc}} V_{an}$$
$$T_{bn} = \frac{T_s}{V_{dc}} V_{bn} \qquad (1)$$
$$T_{cn} = \frac{T_s}{V_{dc}} V_{cn}$$

Where V_{an} , V_{bn} and V_{cn} are the sampled phase voltages and T_{an} , T_{bn} and T_{cn} are the corresponding imaginary switching times [4,8]. As these times could be negative when corresponding voltages are negative, these are known as imaginary switching times. The active voltage vector switching times T_1 and T_2, if the reference voltage vector falls in sector-1 may be expressed as follows [8]:

$$T_1 = T_{an} - T_{bn}$$
$$T_2 = T_{bn} - T_{cn} \qquad (2)$$

In the CSVPWM algorithm, when the reference voltage vector falls in the first sector, V_{an} has a maximum value, V_{cn} has the minimum value and V_{bn} has the middle value. Corresponding to these phase voltages, the imaginary switching time which is proportional to the a-phase (T_{an}) has a maximum value, the imaginary switching time which is proportional to the c-phase (T_{cn}) has a minimum value and the imaginary switching time which is proportional to the b-phase (T_{bn}) is middle value. Thus, in general the active vector switching times T_1 and T_2 may be expressed as

$$T_1 = T_{\max} - T_{mid}$$
$$T_2 = T_{mid} - T_{\min} \qquad (3)$$

The zero voltage vectors switching time is calculated as

$$T_Z = T_s - T_1 - T_2 \qquad (4)$$

The switching sequence of CSVPWM algorithm is $0.5T_z$ - T_1 - T_2 - $0.5T_z$. However, by utilizing the freedom in division of zero state time BBCPWM algorithms can be generated. To generate the BBCPWM algorithms, the zero state time will be shared unequally between two zero states as xT_z for V_0 and $(1-x)T_z$ for V_7 respectively. If x =0.5, then the CSVPWM algorithm is obtained. When x =0, any one of the phases is clamped to positive dc bus for 120 degrees over a fundamental interval and 7-2-1 sequence is obtained. When x =1, any one of the phases is clamped to negative dc bus for 120 degrees over a fundamental interval and 0-1-2 sequence is obtained.

Then by utilizing the concept of active voltage vector time division, various space vector based basic bus-clamping PWM algorithms can be generated. The existing basic bus-clamping PWM (BBCPWM) algorithm uses only one zero state and the advanced BCPWM (ABCPWM) sequences use one zero state and active state division also. The ABCPWM algorithms can be divided into two groups. In one group, the switching sequence will start with zero state, whereas in the other group, the switching sequence will be started with the active state. The sequences of all the possible switching sequences in six sectors are listed in Table-1.

Table 1: Sequences of various possible PWM algorithms

Sector	CSV PWM	BBC PWM		ABC PWM			
I	0127-7210	012-210	721-127	0121-1210	7212-2127	1012-2101	2721-1272
II	0327-7230	032-230	723-327	0323-3230	7232-2327	3032-2303	2723-3272
III	0347-7430	034-430	743-347	0343-3430	7434-4347	3034-4303	4743-3474
IV	0547-7450	054-450	745-547	0545-5450	7454-4547	5054-4505	4745-5474
V	0567-7650	056-650	765-567	0565-5650	7656-6567	5056-6505	6765-5676
VI	0167-7610	016-610	761-167	0161-1610	7616-6167	1016-6101	6761-1676

III. Analysis of RMS Current Ripple

In the space vector approach, the required reference voltage vector is developed in the average manner but not in an instantaneous manner. When the voltage vector is applied to the motor, the current is flowing in the stator winding of the induction motor. The actual value of the stator voltage differs from the applied voltage. Hence, there is always an instantaneous error voltage vector. The error voltage vector is defined as given in (5)

$$V_{rip} = V_k - V_{ref} \qquad (5)$$

where 'k' is the k[th] voltage vector and it take any value from zero to seven. Fig. 1 shows the ripple voltage vectors for the given applied voltage vectors when the reference voltage vector lies in sector I.

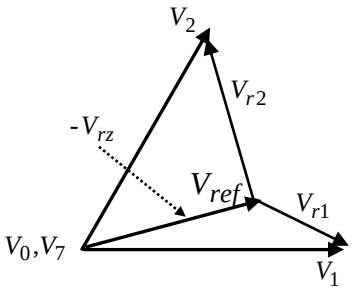

Fig. 1 voltage ripple vectors in sector I

Then, it is possible to define the current ripple vector as defined in (6) [6]

$$i_{rip} = \frac{1}{\sigma L_s} \int_0^t V_{rip} dt \qquad (6)$$

Then the current ripple vectors are given by as follows:

$$i_{r1} = \frac{V_1 - V_{ref}}{\sigma L_s} T_1 \qquad (7)$$

$$i_{r2} = \frac{V_2 - V_{ref}}{\sigma L_s} T_2 \qquad (8)$$

Published By:
Blue Eyes Intelligence Engineering
and Sciences Publication (BEIESP)

$$i_{rz} = -\frac{V_{ref}}{\sigma L_s} T_z \qquad (9)$$

where σ is the leakage coefficient of the induction motor and L_s is the stator inductance. The current ripple vectors can be represented in terms of imaginary switching times as given in (10)-(12).

$$i_{r1} = i_d + j i_{q1} \qquad (10)$$

$$i_{r2} = i_d + j i_{q2} \qquad (11)$$

$$i_{rz} = -j \frac{T_z}{\sigma L_s} \frac{2 M_i V_{dc}}{\pi} = -j i_{qz} \qquad (12)$$

where M_i is the modulation index and defined as

$$M_i = \frac{\pi V_{ref}}{2 V_{dc}} \qquad (13)$$

$$i_d = \frac{T_1}{\sigma L_s}\left(\frac{\pi V_{dc}}{3\sqrt{3} M_i}\frac{T_2}{T_s}\right) \qquad (14)$$

$$i_{q1} = \frac{T_1}{\sigma L_s}\left(\frac{2V_{dc}\pi(T_1 + 0.5T_2)}{9 M_i T_s} - \frac{2V_{dc} M_i}{\pi}\right) \qquad (15)$$

$$i_{q2} = \frac{T_2}{\sigma L_s}\left(\frac{2V_{dc}\pi(0.5T_1 + T_2)}{9 M_i T_s} - \frac{2V_{dc} M_i}{\pi}\right) \qquad (16)$$

The variation of stator current ripple for the corresponding voltage ripple vectors can be derived from (7) - (9). Then, these current ripple variations can be resolved along the d- and q-axes as shown in Fig. 2 - Fig. 6.

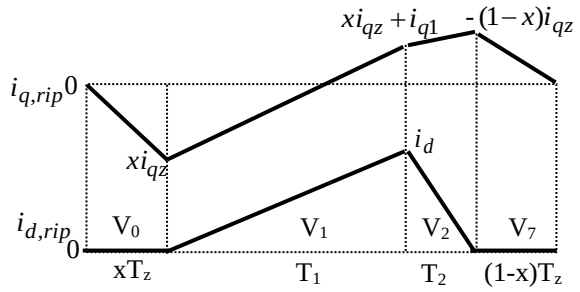

Fig. 2 d-axis and q-axis current ripple variations for 0127, 012 and 721 sequences

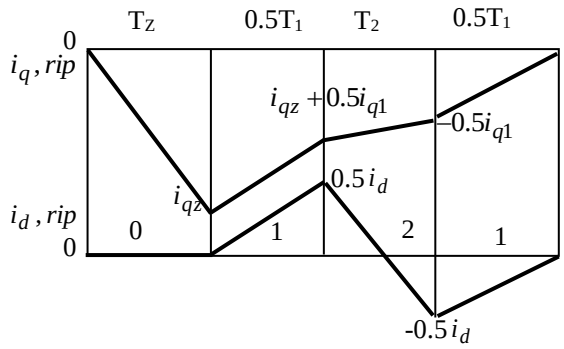

Fig. 3 d-axis and q-axis current ripple variations for 0121 sequence

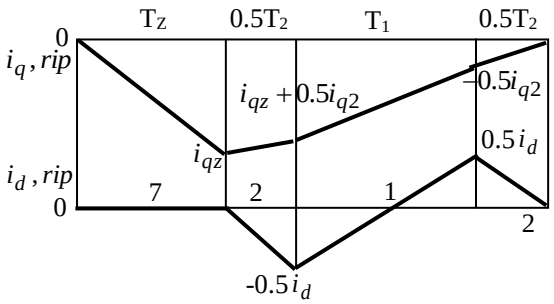

Fig. 4 d-axis and q-axis current ripple variations for 7212 sequence

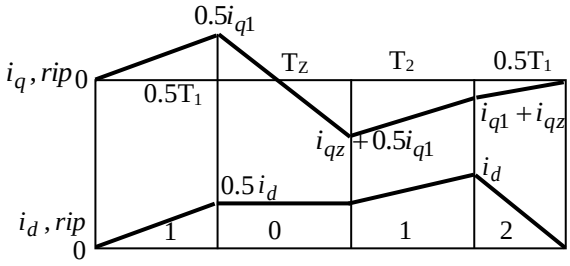

Fig. 5 d-axis and q-axis current ripple variations for 1012 sequence

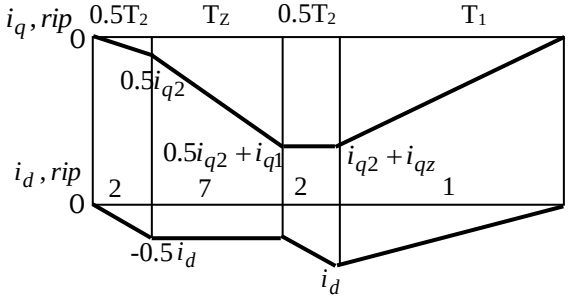

Fig. 6 d-axis and q-axis current ripple variations for 2721 sequence

The q-axis, d-axis and the total rms current ripple over a sampling time interval (T_s) can be evaluated as follows:

$$i_{q,rms}^2 = \frac{1}{T_s}\int_0^{T_s} i_{q,rip}^2\, dt \qquad (17)$$

$$i_{d,rms}^2 = \frac{1}{T_s}\int_0^{T_s} i_{d,rip}^2\, dt \qquad (18)$$

$$i_{rms}^2 = i_{q,rms}^2 + i_{d,rms}^2 \qquad (19)$$

By using (19), the rms current ripple expressions for CSVPWM and existing BBCPWM algorithms can be given as in (20).

$$i_{rms}^2 = \frac{1}{3}\left\{\begin{array}{l} x i_{q0}^2 \frac{xT_z}{T_s} + \left[x i_{qz}^2 + (i_{qz}+i_{q1})^2 + i_{qz}(i_{qz}+i_{q1})\right]\frac{T_1}{T_s} + \\ \left[(i_{qz}+i_{q1})^2 - (1-x) i_{qz}(i_{qz}+i_{q1}) + ((1-x) i_{qz})^2\right]\frac{T_2}{T_s} + \\ ((1-x) i_{qz})^2 \frac{T_7}{T_s} + i_d^2 \frac{(T_1+T_2)}{T_s} \end{array}\right\} \qquad (20)$$

For $x = 0.5$, the rms ripple expression for CSVPWM algorithm is obtained. Similarly when $x = 0$ and $x = 1$, the rms current ripple expressions

Published By:
Blue Eyes Intelligence Engineering
and Sciences Publication (BEIESP)

for existing BBCPWM algorithms can be obtained.

$$i^2_{rms,0121} = \frac{1}{3}\left\{\begin{array}{l} i^2_{qz}\frac{T_z}{T_s} + \\ \left[i^2_{qz} + i_{qz}(i_{qz}+0.5i_{q1}) + (i_{qz}+0.5i_{q1})^2\right]\frac{T_1}{2T_s} + \\ \left[(i_{qz}+0.5i_{q1})^2 - (i_{qz}+0.5i_{q1})0.5i_{q1} + (0.5i_{q1})^2\right]\frac{T_2}{T_s} + \\ (0.5i_{q1})^2\frac{T_1}{2T_s} + (0.5i_d)^2\frac{(T_1+T_2)}{T_s} \end{array}\right\} \quad (21)$$

$$i^2_{rms,7212} = \frac{1}{3}\left\{\begin{array}{l} i^2_{qz}\frac{T_z}{T_s} + \left[i^2_{qz} + i_{qz}(i_{qz}+0.5i_{q2}) + (i_{qz}+0.5i_{q2})^2\right]\frac{T_2}{2T_s} \\ \quad + \left[(i_{qz}+0.5i_{q2})^2 - (i_{qz}+0.5i_{q2})0.5i_{q2} + (0.5i_{q2})^2\right]\frac{T_1}{T_s} \\ \quad + (0.5i_{q2})^2\frac{T_2}{2T_s} + (0.5i_d)^2\frac{(T_1+T_2)}{T_s} \end{array}\right\} \quad (22)$$

$$i^2_{rms,1012} = \frac{1}{3}\left\{\begin{array}{l} (0.5i_{q1})^2\frac{T_1}{2T_s} \\ \quad + \left[(0.5i_{q1})^2 + 0.5i_{q1}(0.5i_{q1}+i_{qz}) + (0.5i_{q1}+i_{qz})^2\right]\frac{T_z}{T_s} \\ \quad + \left[(0.5i_{q1}+i_{qz})^2 + (0.5i_{q1}+i_{qz})(i_{q1}+i_{qz}) + (i_{q1}+i_{qz})^2\right]\frac{T_1}{2T_s} \\ \quad + (i_{q1}+i_{qz})^2\frac{T_2}{T_s} + i_d^2\frac{(T_1+T_2)}{T_s} + (0.5i_d)^2\frac{T_z}{T_s} \end{array}\right\} \quad (23)$$

$$i^2_{rms,2721} = \frac{1}{3}\left\{\begin{array}{l} (0.5i_{q2})^2\frac{T_2}{2T_s} \\ \quad + \left[(0.5i_{q2})^2 + 0.5i_{q2}(0.5i_{q2}+i_{qz}) + (0.5i_{q2}+i_{qz})^2\right]\frac{T_z}{T_s} \\ \quad + \left[(0.5i_{q2}+i_{qz})^2 + (0.5i_{q2}+i_{qz})(i_{q2}+i_{qz}) + (i_{q2}+i_{qz})^2\right]\frac{T_2}{2T_s} \\ \quad + (i_{q2}+i_{qz})^2\frac{T_1}{T_s} + i_d^2\frac{(T_1+T_2)}{T_s} + (0.5i_d)^2\frac{T_z}{T_s} \end{array}\right\} \quad (24)$$

The number of switchings of the CSVPWM and ABCPWM sequences in a sampling time interval (T_s) are three but for the existing BBCPWM algorithms are two. Hence, to get the same average switching frequency of the inverter, a sampling time interval is taken as $T_s = T$ for the CSVPWM and ABCPWM algorithms, while $T_s = (2T/3)$ for the BBCPWM algorithms. Thus the proposed method of analysis is capable of estimating d-axis and q-axis stator current ripples individually. The THD of the stator current waveform is equally affected by the d-axis and q-axis stator current ripples. On the other hand, torque pulsation mainly depends on q-axis current ripple, and is practically independent of d-axis stator current ripple. Thus, the reduction in q-axis ripple signifies the reduction of THD and torque pulsation, while the reduction in d-axis stator current ripple implies reduction in THD only. By using (20) - (24), the rms stator current ripple trajectories over a sixty degrees period for every PWM sequence at a given modulation index are plotted as shown in from Fig. 7 to Fig. 10.

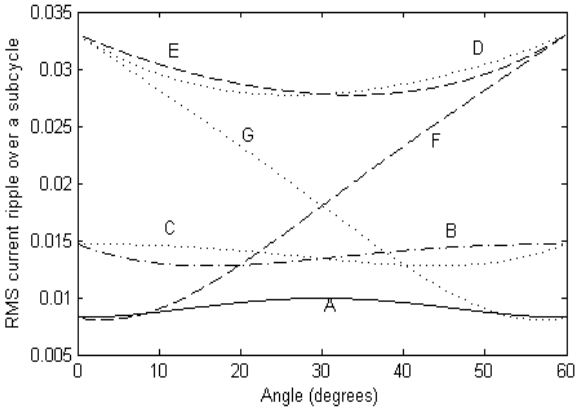

Fig. 7 current ripple trajectories over a sixty degrees period (for one sector) at a modulation index of 0.4 (A=0127, B=012, C=721, D=0121, E=7212, F=1012 and G= 2721)

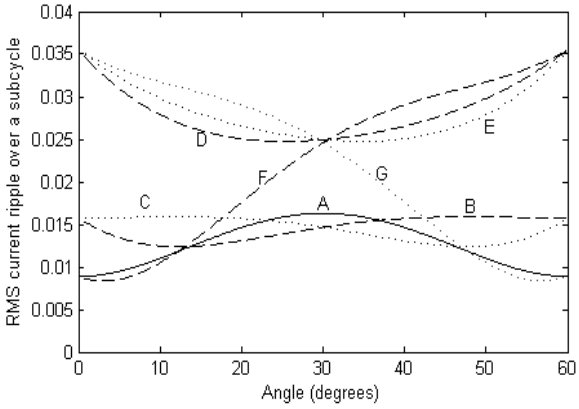

Fig. 8 current ripple trajectories over a sixty degrees period (for one sector) at a modulation index of 0.6 (A=0127, B=012, C=721, D=0121, E=7212, F=1012 and G= 2721)

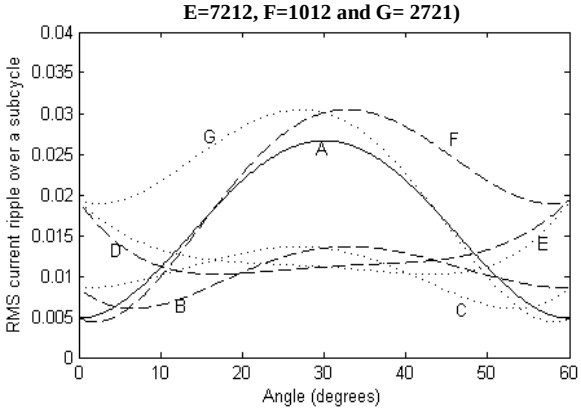

Fig. 9 current ripple trajectories over a sixty degrees period (for one sector) at a modulation index of 0.8 (A=0127, B=012, C=721, D=0121, E=7212, F=1012 and G= 2721)

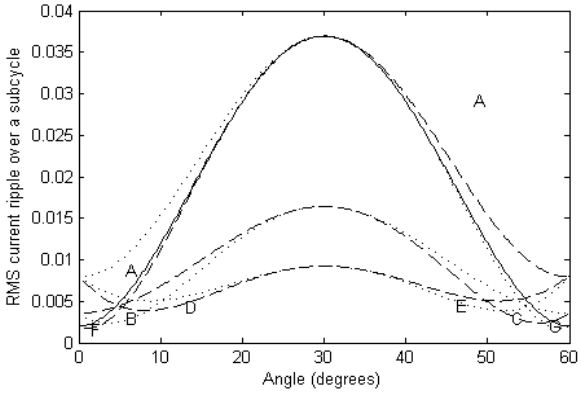

Fig. 10 current ripple trajectories over a sixty degrees period (for one sector) at a modulation index of 0.906 (A=0127, B=012, C=721, D=0121, E=7212, F=1012 and G= 2721)

IV. PROPOSED HPWM ALGORITHM

The proposed HPWM algorithm has been developed by using the rms current ripple analysis of various PWM sequences. From Fig. 7 to Fig. 10, it can be observed that replacing of α by $(60^o - \alpha)$ in the rms current ripple expression of CSVPWM sequence does not change their values. Thus for a given

Published By:
Blue Eyes Intelligence Engineering and Sciences Publication (BEIESP)

sampling time and M_i, 0127 sequence produces equal mean square stator flux ripple at spatial angles α and $(60^o - \alpha)$.

Whereas for the other sequences the mean square flux ripple at α is equal to the mean square stator flux ripple of their respective complimentary sequences at $(60^o - \alpha)$. For a given values of M_i and T_s, these can be given as follows:

$$i^2_{rms,012}(\alpha) = i^2_{rms,721}(60^o - \alpha) \quad (25)$$

$$i^2_{rms,0121}(\alpha) = i^2_{rms,7212}(60^o - \alpha) \quad (26)$$

$$i^2_{rms,1012}(\alpha) = i^2_{rms,2721}(60^o - \alpha) \quad (27)$$

Hence, from the above discussion it can be concluded that the complimentary sequences for 012 and 0121 are 721 and 7212 respectively. By comparing the rms current ripple trajectories of all possible PWM sequences 0127, 012, 721, 0121, 7212, 1012 and 2721 with respective to each other, the zones of superior performance of each sequence can be identified. By considering various combinations, various HPWM algorithms can be generated. However, the proposed HPWM algorithm uses all possible switching sequences. The development of HPWM techniques for reduced current ripple involves determination of superior performance for every sequence. The zone of superior performance for a given sequence is the spatial zone within a sector where the given sequence results in less mean square current ripple than other sequences considered. Thus, the proposed HPWM algorithm is a 7-zone PWM algorithm as shown in Fig. 11, which uses six basic bus-clamping PWM algorithms along with the CSVPWM algorithm for reduced steady state current ripple.

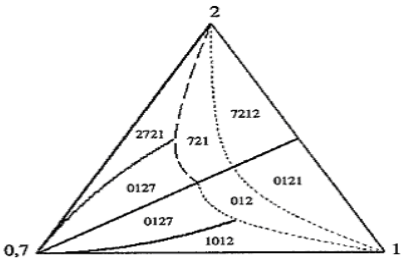

Fig. 11 Zones of superior performance in the proposed HPWM algorithm

V. Proposed HPWM Algorithm Based Vector Controlled Induction Motor Drive

The block diagram proposed HPWM algorithm based vector controlled induction motor drive is as shown in Fig. 12. The actual stator current components i_{ds} and i_{qs}, which are in synchronously rotating reference frame are compared with the reference stator current components i^*_{ds} and i^*_{qs} to generate the errors in current components. From these errors, the reference voltage signals V^*_{ds} and V^*_{qs} can be generated through PI controllers. These reference voltages are then converted into stationary reference frame and given to HPWM block. In HPWM block the two phase voltages are then converted into the three-phase voltages and then the gating pulses will be generated according to the proposed algorithm and given to the voltage source inverter.

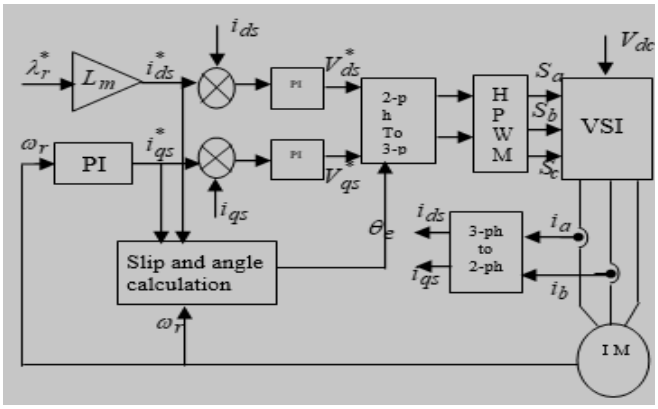

Fig. 12 Block diagram of proposed indirect vector control Method

VI. Simulation Results and Discussion

To verify the proposed HPWM algorithm based vector controlled induction motor drive, the numerical simulation studies have been carried out using Matlab-simulink. For the simulation, the average switching frequency of the inverter is taken as 5 kHz. The induction motor used in this paper is a 4 kW, 400V, 1470 rpm, 4-pole, 50 Hz, 3-phase induction motor having the following parameters: R_s= 1.57Ω, R_r = 1.21Ω, L_s = 0.17H, L_r = 0.17H, L_m = 0.165 H and J = 0.089 Kg.m^2.

The simulation results of CSVPWM based vector controlled induction motor drive are shown in Fig. 13 – Fig. 18. The simulation results of proposed HPWM based vector controlled induction motor drive are given from Fig. 19 – Fig. 24. From the simulation results, it can be observed that, the proposed HPWM algorithm gives reduced steady state current and torque ripples. Moreover, the proposed algorithm gives reduced harmonic distortion when compared with the CSVPWM algorithm. Moreover, from the line current harmonic spectra corresponding to CSVPWM algorithm, it can be observed that the harmonic components are around frequencies that are integral multiples of the switching frequency (5 kHz). On the other hand, the proposed HPWM algorithm gives spread spectra. Hence, the proposed HPWM algorithm also reduces the acoustical noise of the induction motor with a uniform sampling frequency.

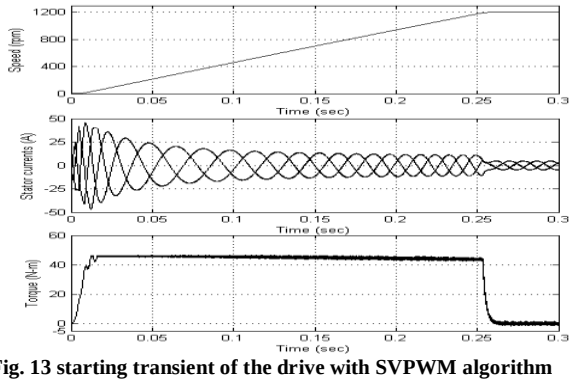

Fig. 13 starting transient of the drive with SVPWM algorithm

Published By:
Blue Eyes Intelligence Engineering
and Sciences Publication (BEIESP)

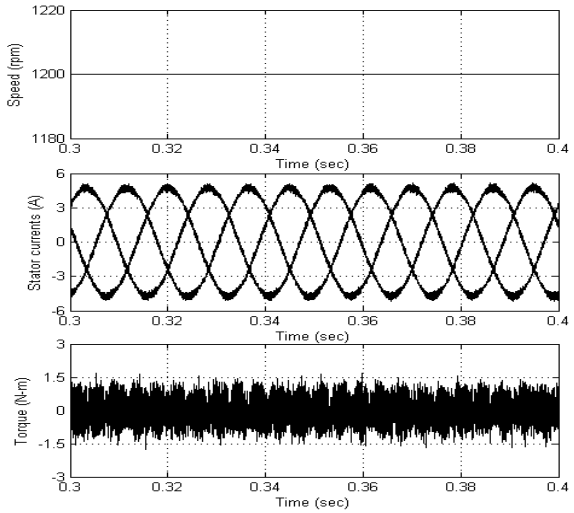

Fig. 14 steady state plots of the drive with SVPWM algorithm

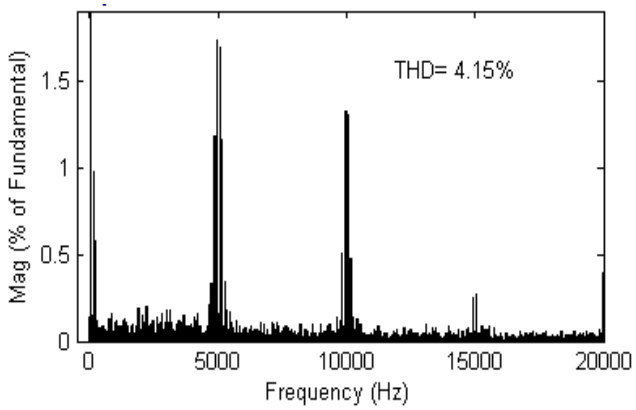

Fig. 15 Harmonic spectra of line current with the SVPWM algorithm

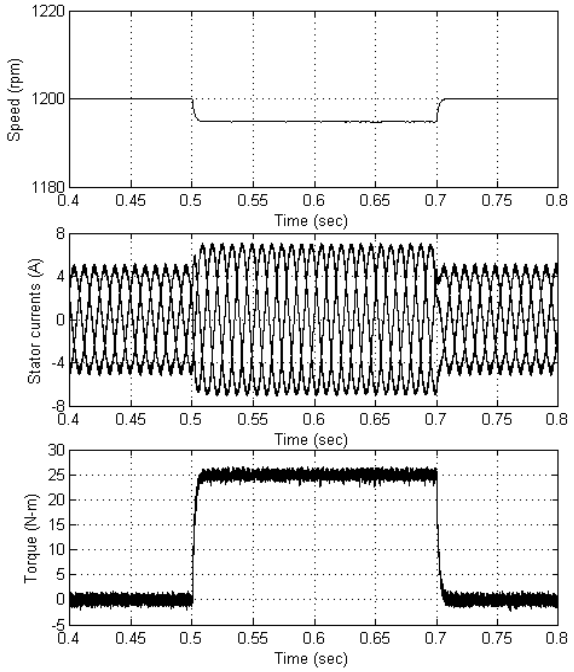

Fig. 16 transients of the induction motor drive with SVPWM algorithm during step change in load

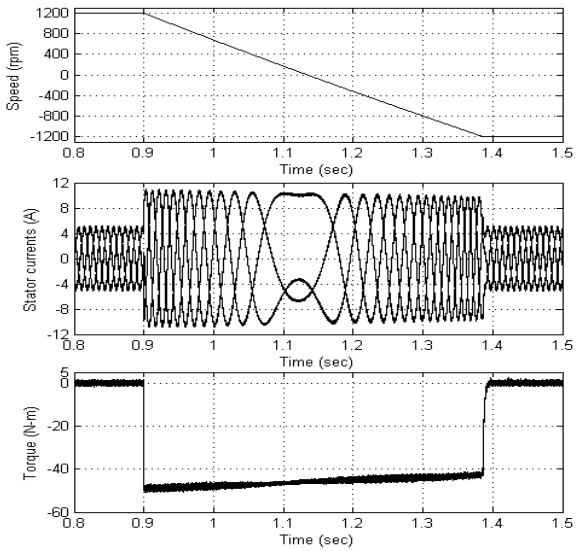

Fig. 17 transients of the induction motor drive with SVPWM algorithm during speed reversal (1200 RPM to -1200RPM)

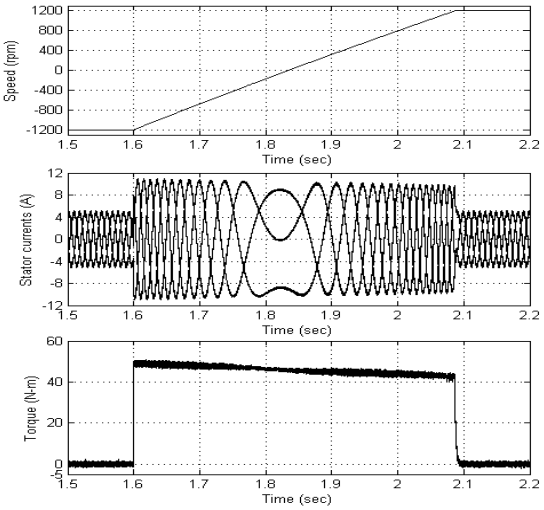

Fig. 18 transients of the induction motor drive with SVPWM algorithm during speed reversal (-1200 RPM to 1200RPM)

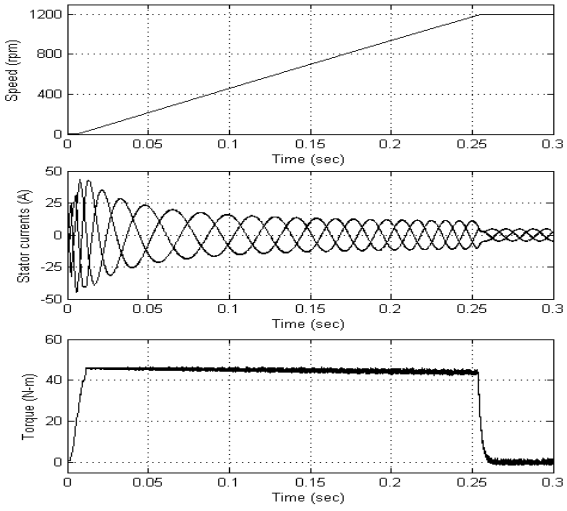

Fig. 19 starting transient of the drive with proposed HPWM algorithm

Published By:
Blue Eyes Intelligence Engineering and Sciences Publication (BEIESP)

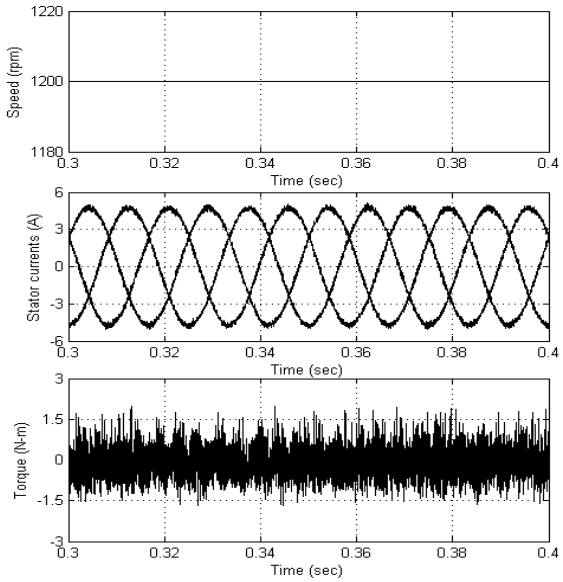

Fig. 20 steady state plots of the drive with proposed HPWM algorithm

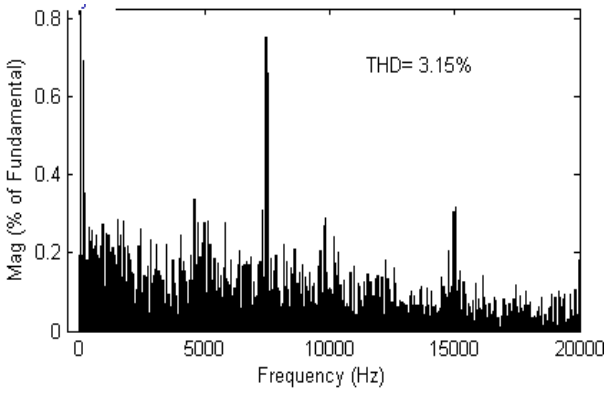

Fig. 21 Harmonic spectra of line current with proposed HPWM algorithm

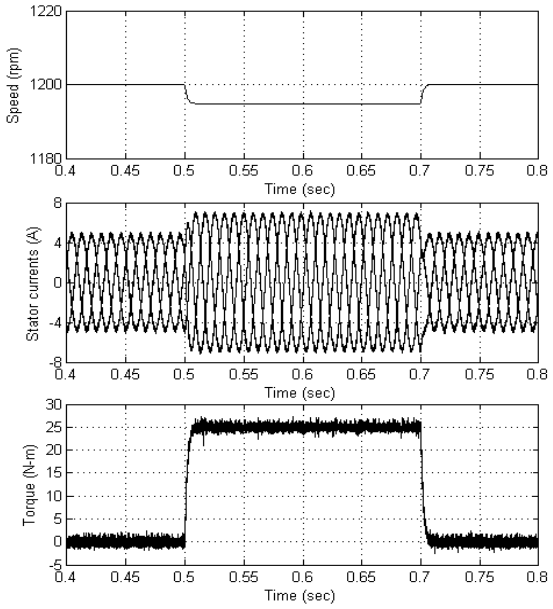

Fig. 22 transients of the induction motor drive with proposed HPWM algorithm during step change in load

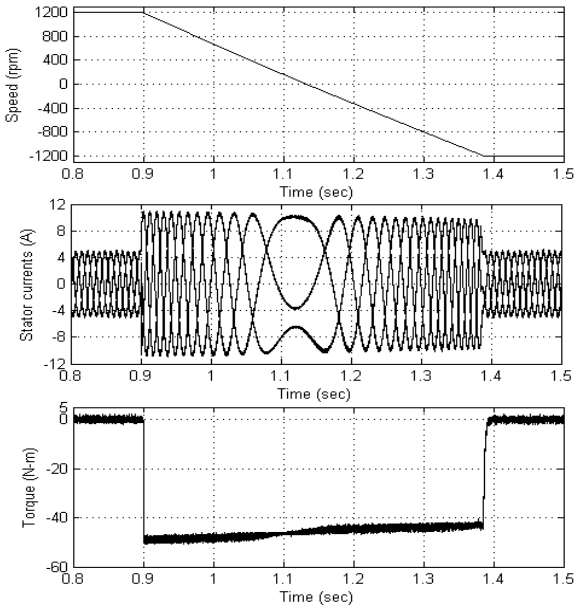

Fig. 23 transients of the induction motor drive with proposed HPWM algorithm during speed reversal (1200 RPM to -1200RPM)

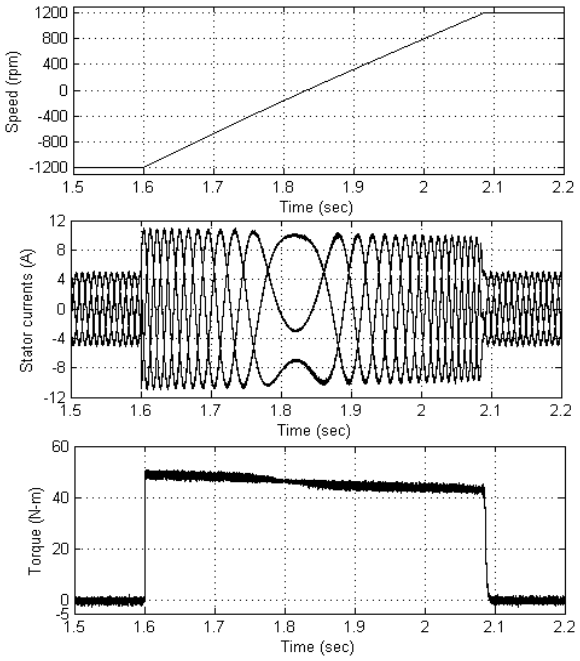

Fig. 24 transients of the induction motor drive with proposed HPWM algorithm during speed reversal (-1200 RPM to 1200RPM)

Thus, the proposed HPWM algorithm reduces the steady state current ripple and acoustical noise of the induction motor when compared with the CSVPWM algorithm. Moreover, the proposed HPWM algorithm gives superior performance at all modulation indices when compared with the conventional SVPWM algorithm.

VII. CONCLUSIONS

The analysis of rms current ripple for various PWM switching sequences has been given and graphically represented. From these rms ripple expressions, the proposed HPWM algorithm has

Published By:
Blue Eyes Intelligence Engineering and Sciences Publication (BEIESP)

been developed for Hybrid PWM Algorithm Based Vector Controlled Induction Motor Drive to Achieve Superior Waveform Quality.

The proposed HPWM algorithm selects a suitable switching sequence that results in reduced current ripple in every sampling time interval. From the simulation results, it can be observed that the proposed HPWM algorithm gives less THD when compared with the CSVPWM algorithm. Moreover, as the HPWM gives spread spectra, it reduces the acoustical noise of the induction motor with a uniform sampling frequency. Hence, to reduce the acoustical noise, special methods with random sampling frequencies are not necessary. Thus, the proposed HPWM algorithm gives superior performance at all modulation indices.

REFERENCES

1. F. Blaschke "The principle of field orientation as applied to the new transvector closed loop control system for rotating-field machines," *Siemens Review*, 1972, pp 217-220.
2. Heinz Willi Vander Broeck, Hnas-Christoph Skudelny and Georg Viktor Stanke, "Analysis and realization of a pulsewidth modulator based on voltage space vectors" *IEEE Trans. Ind. Applicat.*, vol. 24, no. 1, Jan/Feb 1988, pp. 142-150.
3. Ahmet M. Hava, Russel J. Kerkman and Thomas A. Lipo, "Simple analytical and graphical methods for carrier-based PWM-VSI drives" *IEEE Trans. Power Electron.* vol. 14, no. 1, Jan 1999, pp. 49-61.
4. Dae-Woong Chung, Joohn-Sheok Kim and Seung-Ki Sul, "Unified voltage modulation technique for real-time three-phase power conversion" *IEEE Trans. Ind. Applicat.*, vol. 34, no. 2, Mar/Apr 1998, pp. 374-380
5. G.Narayanan , Di Zhao, H. Krishnamurthy and Rajapandian Ayyanar, "Space vector based hybrid techniques for reduced current ripple" *IEEE Trans. Ind. Applic.*, Vol.55, No.4, pp.1614-1626, April 2008.
6. D. Casadei, G. Serra, A. Tani, and L. Zarri, "theoretical and experimental analysis for the RMS current ripple Minimization in induction motor drives controlled by SVM technique" IEEE Trans. Ind. Electron., vol.51, no.5, pp.1056,-1065, Oct, 2004.
7. Di Zhao, V.S.S. Pavan Kumar Hari, G. narayanan and R, Ayyanar, "space-vector-based hybrid Pulsewidth modulation techniques for reduced harmonic distortion and switching losses" IEEE. Trans. Power Electron., vol.25, no.3, pp.760-774, March, 2010.
8. T. Brahmananda Reddy, J. Amarnath and D. Subbarayudu, "Improvement of DTC performance by using hybrid space vector Pulsewidth modulation algorithm" International Review of Electrical Engineering, Vol.4, no.2, pp. 593-600, Jul-Aug, 2007.

AUTHOR PROFILE

K. Satyanarayana has obtained the A.M.I.E degree in Electrical Engineering from Institution of Engineers (India) in 1996 and the M.Tech degree in Power Electronics from JNTU College of Engineering, Hyderabad in 2003. He is presently working as Professor and H.O.D. in the Department of Electrical and Electronics Engineering, Pragati Engineering College, Surampalem, Peddapuram, A.P., INDIA. He is presently pursuing Doctoral degree from J.N.T.U. College of Engineering, Kakinada. He presented many research papers in various national and international journals and conferences. His research interests include Power Electronic Drives, Multilevel inverters, FWM and Vector Control techniques.

Dr. J.Amarnath graduated from Osmania University in the year 1982, M.E from Andhra University in the year 1984 and Ph.D from J.N.T. University, Hyderabad in the year 2001. He is presently Professor in the Department of Electrical and Electronics Engineering, JNTU College of Engineering, Hyderabad, India. He presented more than 200 research papers in various national and international conferences and journals. His research areas include Gas Insulated Substations, High Voltage Engineering, Power Systems and Electrical Drives.

Dr.A.Kailasa Rao has graduated from IIT, Kharagpur in Electrical Engineering**.** He took his M.Tech degree in Power Systems from JNTU, Hyderabad and obtained Ph.D**,**from IIT, Kharagpur in Control Systems. He has Published many research papers, all in International Journals. A research monograph based on his Ph.D Thesis work is published by Springer Verlag, New York.He has worked as lecturer, Assistant - Professor, Professor and HOD, Vice-Principal and Principal in JNTU College of Engineering, Kakinada..He has also worked in the JNTU University Head Quarters, Hyderabad in various capacities as Professor in P.G School, coordinator of Examination Reforms Unit and Director, CARD (Career Advancement, Research and Development).Currently, he is a Professor and Director of Pragati Engineering College, Surampalem**,** Andhra Pradesh, INDIA.

Published By:
Blue Eyes Intelligence Engineering and Sciences Publication (BEIESP)